Aromatase Excess Syndrome: Identification of Cryptic Duplications and Deletions Leading to Gain of Function of *CYP19A1* and Assessment of Phenotypic Determinants

Maki Fukami, Makio Shozu, Shun Soneda, Fumiko Kato, Akemi Inagaki, Hiroshi Takagi, Keiichi Hanaki, Susumu Kanzaki, Kenji Ohyama, Tomoaki Sano, Toshinori Nishigaki, Susumu Yokoya, Gerhard Binder, Reiko Horikawa, and Tsutomu Ogata

Department of Molecular Endocrinology (M.F., S.S., F.K., T.O.), National Research Institute for Child Health and Development, Tokyo 157-8535, Japan; Department of Reproductive Medicine (M.S.), Graduate School of Medicine, Chiba University, Chiba 206-8670, Japan; Department of Diabetes and Endocrinology (A.I., H.T.), Nagoya Second Red Cross Hospital Nagoya 466-8650, Japan; Department of Women's and Children's Family Nursing (K.H.) and Division of Pediatrics and Perinatology (S.K.), Tottori University, Yonago 683-8503, Japan; Department of Pediatrics (K.O., T.S.), Interdisciplinary Graduate School of Medicine and Engineering, University of Yamanashi, Chuo 408-3898, Japan; Department of Pediatrics (T.N.), Osaka Police Hospital, Osaka 543-0035, Japan; Department of Medical Subspecialties (S.Y., R.H.), National Medical Center for Children and Mothers, Tokyo 157-8535, Japan; and Pediatric Endocrinology Section (G.B.), University Children's Hospital, Tuebingen 72076, Germany

Context: Aromatase excess syndrome (AEXS) is a rare autosomal dominant disorder characterized by gynecomastia. Although cryptic inversions leading to abnormal fusions between *CYP19A1* encoding aromatase and its neighboring genes have been identified in a few patients, the molecular basis remains largely unknown.

Objective: The objective of the study was to examine the genetic causes and phenotypic determinants in AEXS.

Patients: Eighteen affected males from six families participated in the study.

Results: We identified three types of heterozygous genomic rearrangements, *i.e.* a 79,156-bp tandem duplication involving seven of 11 noncoding *CYP19A1* exons 1, a 211,631-bp deletion involving exons 2–43 of *DMXL2* and exons 5–10 of *GLDN*, and a 165,901-bp deletion involving exons 2–43 of *DMXL2*. The duplicated exon 1 functioned as transcription start sites, and the two types of deletions produced the same chimeric mRNA consisting of *DMXL2* exon 1 and *CYP19A1* coding exons. The *DMXL2* exon 1 harbored a translation start codon, and the *DMXL2/CYP19A1* chimeric mRNA was identified in only 2–5% of *CYP19A1*-positive transcripts. This was in contrast to the inversion-mediated chimeric mRNA that had no coding sequence on the fused exon 1 and accounted for greater than 80% of *CYP19A1*-positive transcripts. *CYP19A1* was expressed in a limited number of tissues, whereas its neighboring genes involved in the chimeric mRNA formation were expressed widely.

Conclusions: This study provides novel mechanisms leading to gain of function of *CYP19A1*. Furthermore, it appears that clinical severity of AEXS is primarily determined by the tissue expression pattern of relevant genes and by the structural property of promoter-associated exons of chimeric mRNA. ***(J Clin Endocrinol Metab* 96: E1035–E1043, 2011)**

ISSN Print 0021-972X ISSN Online 1945-7197
Printed in U.S.A.

doi: 10.1210/jc.2011-0145 Received January 18, 2011. Accepted March 22, 2011.
First Published Online April 6, 2011

Abbreviations: AEXS, Aromatase excess syndrome; CGH, comparative genomic hybridization; E_2, estradiol; FISH, fluorescence *in situ* hybridization; hCG, human chorionic gonadotropin; LCL, lymphoblastoid cell line; NMD, nonsense-mediated mRNA decay; RACE, rapid amplification of cDNA ends; SF, skin fibroblast; T, testosterone.

Aromatase is a cytochrome P450 enzyme that plays a crucial role in the estrogen biosynthesis (1). It catalyzes the conversion of Δ4-androstendione into estrone and that of testosterone (T) into estradiol (E_2) in the placenta and ovary as well as in other tissues such as the fat, skin, bone, and brain (1). It is encoded by *CYP19A1* consisting of at least 11 noncoding exons 1 and nine coding exons 2–10 (Supplemental Fig. 1, published on The Endocrine Society's Journals Online web site at http://jcem.endojournals.org) (2, 3). Each exon 1 is accompanied by a tissue-specific promoter and is spliced alternatively onto a common splice acceptor site at exon 2, although some transcripts are known to contain two of the exons 1, probably due to a splice error (2, 4). Of the 11 exons 1, exon I.4 appears to play a critical role in the regulation of estrogen biosynthesis in males because this exon contains a major promoter for extragonadal tissues including the skin and fat (2).

Excessive *CYP19A1* expression causes a rare autosomal dominant disorder known as aromatase excess syndrome (AEXS) (5–8). AEXS is characterized by pre- or peripubertal onset gynecomastia, advanced bone age from childhood to the pubertal period, and short adult height in affected males (5–8). Affected females may show several clinical features such as macromastia, precocious puberty, irregular menses, and short adult height (6–8). In this regard, previous studies have identified four heterozygous cryptic inversions around *CYP19A1* in patients with AEXS (5, 8). Each inversion results in the formation of a chimeric gene consisting of a noncoding exon(s) of a neighboring gene (*CGNL1*, *MAPK6*, *TMOD3*, or *TLN2*) and coding exons of *CYP19A1*. Because this condition is predicted to cause aberrant *CYP19A1* expression in tissues in which each neighboring gene is expressed, such inversions have been regarded to be responsible for AEXS (5, 8).

However, such inversions have been revealed only in a few patients with AEXS, and, despite extensive studies, no other underlying genetic mechanisms have been identified to date (6, 8–10). Here we report novel genomic rearrangements in AEXS and discuss primary phenotypic determining factors in AEXS.

Patients and Methods

Patients

This study was approved by the Institutional Review Board Committee at the National Center for Child Health and Development and was performed after obtaining informed consent. We examined 18 male patients aged 8–69 yr (cases 1–18) from six unrelated families A-F (Fig. 1A). The probands were ascertained by bilateral gynecomastia (Fig. 1B) and the remaining 12 males by familial studies. Ten other males allegedly had gynecomastia. There were four obligatory carrier females.

Phenotypic assessment showed pre- or peripubertal onset gynecomastia in all cases, small testes and fairly preserved masculinization in most cases, obvious or relative tall stature in childhood and grossly normal or relative short stature in adulthood, and age-appropriate or mildly advanced bone ages (Table 1) (for detailed actual data, see Supplemental Table 1). Such clinical features, especially gynecomastia, tended to be milder in cases 1–4 from families A and B than in the remaining cases from families C-F. Fertility or spermatogenesis was preserved in all adult cases (≥20 yr). In addition, the obligatory carrier females from families B and D had apparently normal phenotype, and such females from families E and F exhibited early menarche (9.0 yr) and short adult stature (−2.8 SD), respectively.

Blood endocrine studies revealed that LH values were grossly normal at the baseline and variably responded to GnRH stimulation, whereas FSH values were low at the baseline and responded poorly to GnRH stimulation, even after preceding GnRH priming (Table 1) (for detailed actual data, see Supplemental Table 1) (see also Fig. 1C for the cases aged ≥15 yr). Δ^4-Androstendione, T, and dihydrotestosterone values were low or normal. A human chorionic gonadotropin (hCG) test indicated relatively low but normal T responses in five young cases. In most cases, estrone values were elevated, E_2 values were normal or elevated, and E_2/T ratios were elevated. These endocrine data were grossly similar among cases 1–18.

Aromatase inhibitor (anastrozole, 1 mg/d) was effective in all the four cases treated (Supplemental Table 1) (see also Fig. 1C for cases aged ≥15 yr). Gynecomastia was mitigated within 6 months of treatment, and endocrine data were ameliorated within 1 month of treatment.

Primers

Primers used in this study are shown in Supplemental Table 2.

CYP19A1 mRNA levels and aromatase activities

We analyzed relative mRNA levels of *CYP19A1* and catalytic activities of aromatase in skin fibroblasts (SF) and lymphoblastoid cell lines (LCL). mRNA were extracted by a standard method and were subjected to RT-PCR using a high capacity RNA-to-cDNA kit (Life Technologies, Carlsbad, CA). A relative amount of *CYP19A1* mRNA against *B2M* was determined by the real-time PCR method using the Taqman gene expression assay on ABI PRISM 7500fast (Life Technologies) (assay no. Hs00903411_m1 for *CYP19A1* and Hs99999907_m1 for *B2M*). PCR was performed in triplicate. Aromatase activity was determined by a tritium incorporation assay (11). In brief, the samples were incubated with androstenedione-2-^{3}H for 2 h, and $^3H H_2O$ in the supernatant of the culture media was measured with a scintillation counter LSC-5100 (Aloka, Tokyo, Japan).

Sequence analysis of *CYP19A1*

Leukocyte or SF genomic DNA samples from the six probands and additional four male patients (Fig. 1A) were PCR amplified for the coding exons 2–10 and their flanking splice sites of *CYP19A1*. Subsequently the PCR products were subjected to direct sequencing from both directions on CEQ 8000 autosequencer (Beckman Coulter, Fullerton, CA).

Genome structure analysis

Oligonucleotide array-based comparative genomic hybridization (CGH) analyses were carried out using a custom-built

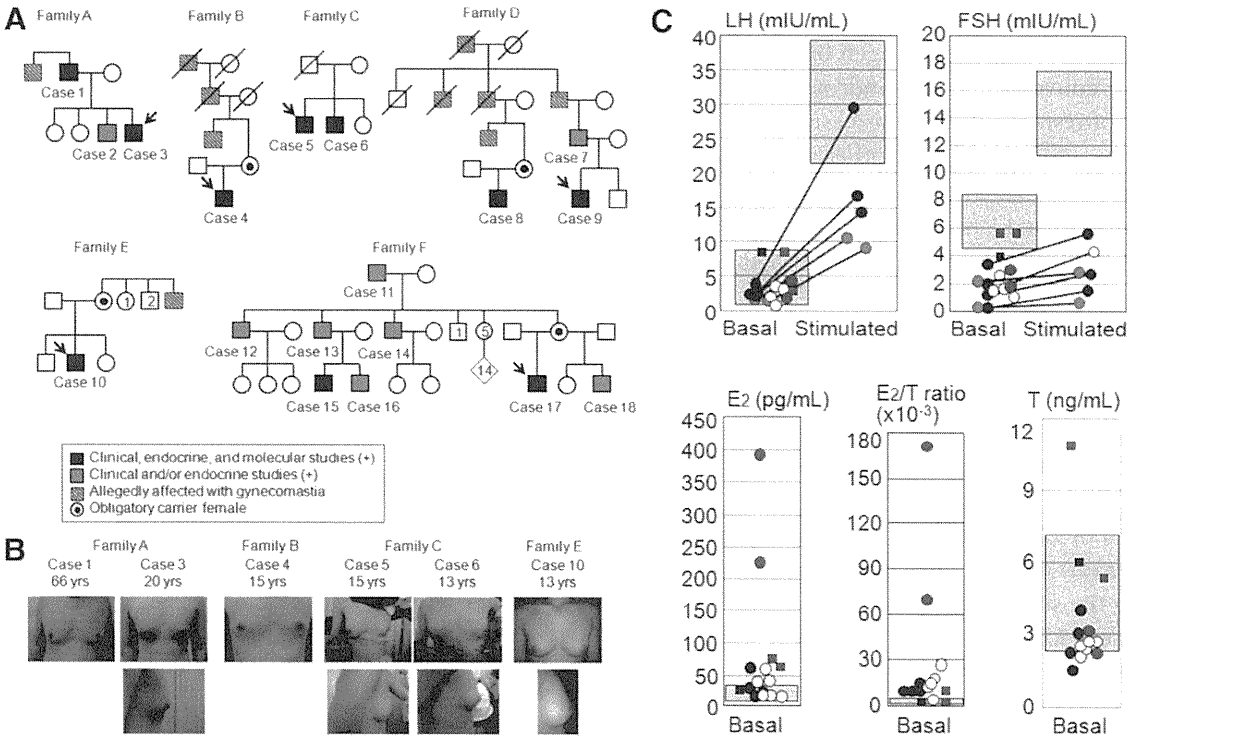

FIG. 1. Summary of clinical data. A, Pedigrees of six families with patients exhibiting AEXS-compatible phenotype. Families A–E are of Japanese origin, and family F is of German origin. Cases from families A–D were hitherto unreported, whereas those from families E and F have previously been described as having AEXS phenotypes (6, 8). B, Gynecomastia of six cases. C, Endocrine data in cases 15 yr of age or older. The *black*, *white*, and *red colors* represent the data in cases of the duplication, the deletion, and the inversion types, respectively; the *blue color* indicates the data of GnRH test after GnRH priming in two cases of the duplication type. The data at the time of diagnosis are denoted by *circles*, and those on aromatase inhibitor (anastrozole) treatment (1 mg/d in the duplication and the deletion types and 2–4 mg/d in the inversion types) are depicted by *squares*. The *light purple areas* represent the normal reference ranges.

oligo-microarray containing 90,000 probes for the 15q11.2-q26.3 region and approximately 10,000 reference probes for other chromosomal region (2 × 105K format, design identification 026533) (Agilent Technologies, Palo Alto, CA). The procedure was as described in the manufacturer's instructions. Fluorescence *in situ* hybridization (FISH) analysis was performed for lymphocyte or SF metaphase spreads, using long PCR products (FISH probes 1 and 2) for rearranged regions and CEP 15 probe for *D15Z4* used as an internal control (Abbott, Abbott Park, IL). The FISH probes 1 and 2 were labeled with digoxigenin and detected by rhodamine antidigoxigenin, and the CEP 15 probe was detected according to the manufacturer's protocol.

Characterization of the duplications and deletions

The duplication junctions were determined by direct sequencing for standard PCR products obtained with a variety of combinations of primers hybridizing to different positions within the *CYP19A1* exons 1 region. The deletion junctions were identified by direct sequencing of the long PCR products obtained with primer pairs flanking the deletions. The sizes of duplications and the deletions were determined by comparing obtained sequences with NT_010194 sequences at the National Center for Biotechnology Information Database (http://www.ncbi.nlm.nih.gov/; Bethesda, MD). The presence or absence of repeat sequences around the breakpoints was examined with Repeatmasker (http://www.repeatmasker.org).

For mRNA analysis, we preformed 5′-rapid amplification of cDNA ends (RACE) using a SMARTER RACE cDNA amplification kit (Takara Bio, Ohtsu, Japan). For both duplications and deletions, first PCR was carried out using the forward primer mix provided in the kit (Universal primer A mix) and an antisense reverse primer specific to *CYP19A1* exon 3 (RACE Rev). Second PCR was carried out for diluted products of the first PCR, using the nested forward primer of the kit (Nested universal primer A) and a reverse primer for *CYP19A1* exon 2 (Nested Rev). For duplications, furthermore, second PCR was also performed using various combinations of primers hybridizing to each *CYP19A1* exon 1. Subsequently PCR products were subcloned into TOPO cloning vector (Life Technologies) and subjected to direct sequencing. Then, the obtained sequences were examined with BLAST Search (National Center for Biotechnology Information). The presence or absence of promoter-compatible sequences was analyzed with the University of California, Santa Cruz, genome browser (http://genome.ucsc.edu/).

Relative mRNA levels of *CYP19A1* and its neighboring genes

We investigated relative mRNA levels of *CYP19A1* and *DMXL2* as well as those of *CGNL1*, *MAPK6*, *TMOD3*, and *TLN2* involved in the previously reported cryptic inversions (5, 8) in various human tissues. In this experiment, cDNA of SF and LCL were obtained from control males, and the remaining human cDNA samples were purchased from Life Technologies or Takara Bio. Relative quantification of mRNA against *TBP* was carried out using Taqman gene expression assay kit

TABLE 1. Summary of clinical studies in male patients with aromatase excess syndrome[a]

	Present study						Previous studies			
	Family A	Family B	Family C	Family D	Family E	Family F	Family 1	Family 2	Sporadic	
Cases	Cases 1–3	Case 4	Cases 5–6	Cases 7–9	Case 10	Cases 11–18	Two cases[b]	Proband[c]	Patient 1	Patient 2
Mutation type	Duplication	Duplication	Deletion	Deletion	Deletion	Deletion	Inversion	Inversion	Inversion	Inversion
Phenotypic findings										
Gynecomastia	Yes (mild)	Yes (mild)	Yes (moderate)	Yes (moderate)	Yes (moderate)	Yes (moderate)	Yes (severe)	Yes (severe)	Yes (severe)	Yes (severe)
Pubertal defect	Yes (mild)	Yes (mild)	Yes (mild)	No	No	Yes (mild)	N.D.	Yes (mild)	No	N.D.
Short adult height	No	No	N.D.	No	N.D.	No	Yes	N.D.	Yes	N.D.
Spermatogenesis	Preserved	N.D.	N.D.	Preserved	N.D.	Preserved	Preserved	N.D.	N.D.	N.D.
Endocrine findings										
LH (basal)	Normal	Normal	Normal	Normal/low	Normal	Normal/low	Normal	Normal/low	Normal	N.E.
LH (GnRH stimulated)[d]	Low	Normal	High	Normal	Normal	Normal	N.E.	Low	N.E.	N.E.
FSH (basal)	Low	Low	Low	Low	Low	Normal/low	Normal/low	Low	Low	N.E.
FSH (GnRH stimulated)[d]	Low	Low	Low	Low	Low	Low	N.E.	Low	N.E.	N.E.
T (basal)	Normal/low	Normal	Normal/low	Normal/low	Normal	Normal/low	Normal	Normal/low	Low	N.E.
T (hCG stimulated)[e]	N.E.	N.E.	Normal	Normal	Normal	Normal	N.E.	Normal	N.E.	N.E.
E_1 (basal)	High	High	N.E.	High	High	High	High	High	High	N.E.
E_2 (basal)	Normal	High	High	Normal	High	Normal/high	High	High	High	N.E.
E_2 to T ratio	High	High	High	High	High	High	High	High	High	N.E.

E_1, Estrone; N.D., not determined; N.E., not examined.

[a] Detailed actual data are shown in Supplemental Table 1.

[b] A father-son pair.

[c] The sister has macromastia, large uterus, and irregular menses; the parental phenotype has not been described.

[d] GnRH 100 $\mu g/m^2$ (maximum 100 μg) bolus iv; blood sampling at 0, 30, 60, 90, and 120 min.

[e] hCG 3000 IU/m^2 (maximum 5000 IU) im for 3 consecutive days; blood sampling on d 1 and 4.

(assay no. Hs00903411_m1 for *CYP19A1*; Hs00324048_m1 for *DMXL2*; Hs00262671_m1 for *CGNL1*; Hs00833126_g1 for *MAPK6*; Hs00205710_m1 for *TMOD3*; Hs00322257_m1 for *TLN2*; and Hs99999910_m1 for *TBP*). The experiments were carried out three times.

Results

CYP19A1 mRNA levels and aromatase activities

Although relative mRNA levels of *CYP19A1* and catalytic activities of aromatase were grossly similar between LCL of case 3 (family A), case 4 (family B), and case 5 (family C) and those of control subjects, they were significantly higher in SF of case 3 (family A), case 4 (family B), case 9 (family D), and case 10 (family E) than in those of control subjects (Fig. 2).

Sequence analysis of *CYP19A1*

Direct sequencing showed no mutation in *CYP19A1* coding exons 2–10 of the 10 cases examined.

Genome structure analysis

CGH analysis revealed heterozygous cryptic duplications involving most of the *CYP19A1* exons 1 region in cases from families A and B, heterozygous cryptic deletions involving most of *DMXL2* and part of *GLDN* in cases from family C, and heterozygous cryptic deletions involving most of *DMXL2* in cases from families D–F (Fig. 3A). FISH analysis supported the duplications and confirmed the deletions.

Characterization of the cryptic duplications

Aberrant PCR products were obtained with the P2 primer (which amplifies a segment between exon I.1 and exon IIa with the P1 primer) and the P3 primer (which amplifies a segment between exon I.2 and exon I.6 with the P4 primer), and sequencing of the PCR products showed the same tandem duplication involving seven of the 11 exons 1 of *CYP19A1* in cases from families A and B (Fig. 3B). The duplicated region was 79,156-bp long, and the

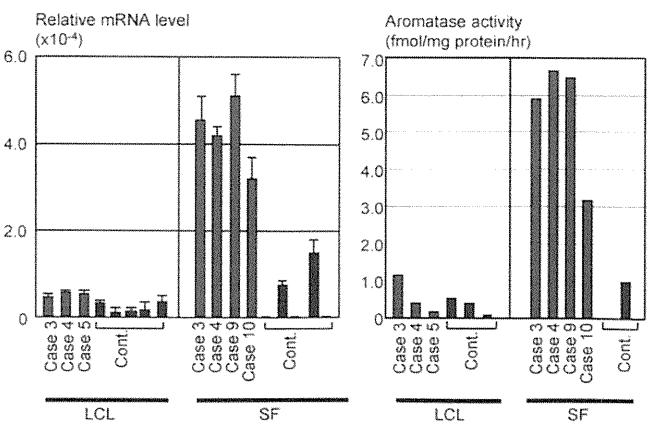

FIG. 2. Relative *CYP19A1* mRNA levels against *B2M* and catalytic activities of aromatase.

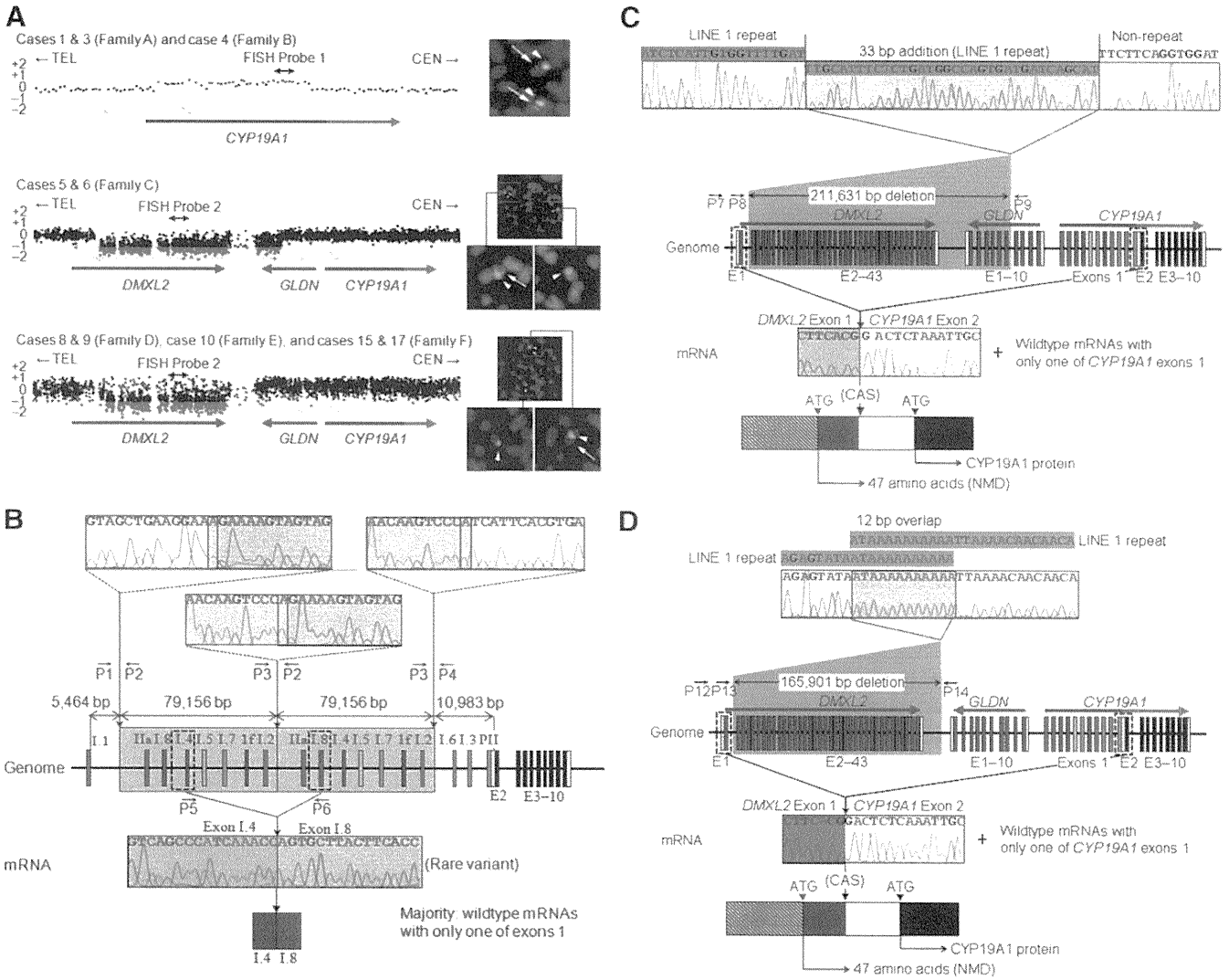

FIG. 3. Summary of molecular studies. For *CYP19A1*, the *dark* and *light blue lines* represent the genomic regions for noncoding exons 1 and coding exons 2–10, respectively. A, Oligoarray CGH and FISH analyses. In CGH analysis, the *black*, *red*, and *green dots* denote signals indicative of the normal, the increased (>+0.5), and the decreased (<−1.0) copy numbers, respectively. In FISH analysis, *two red signals* with an apparently different density are identified in cases from families A and B by FISH probe 1, whereas only a *single red signal* is found in cases from families C–F by FISH probe 2. The *green signals* are derived from the internal control probe. B, Schematic representation of the tandem duplication shared in common by cases 1 and 3 from family A and case 4 from family B. Genome, The junction sequence of the tandem duplication (*yellow boxes*) is shown, together with the original normal sequences at the 5′- and the 3′-ends of the duplicated region. The sequences highlighted with *light green* and *light orange* are identical, and 1 bp (A) is shared at the junction point (highlighted with *light yellow*). mRNA, The sequence of a rare clone is shown. The 3′-end of exon I.4 is connected with the 5′-end of exon I.8. C, Schematic representation of the deletion in sibling cases 5 and 6 from family C. Genome, The junction sequence of the deletion (*a gray area*) is shown. The fusion has occurred between a LINE 1 repeat sequence (*highlighted with blue*) at intron 1 of *DMXL2* and a nonrepeat sequence at intron 4 of *GLDN* and is accompanied by an addition of a 33-bp segment with a LINE 1 repeat sequence. mRNA, The sequence of a rare chimeric gene transcript is shown. *DMXL2* exon 1 consisting of a noncoding region (a *red striped box*) and a coding region (a *red box*) is spliced onto the common acceptor site (CAS) of *CYP19A1* exon 2 comprising an untranslated region (a *white box*) and a coding region (a *black box*). Thus, this transcript has two translation initiation codons (ATG), although the mRNA destined to produce a 47-amino acid protein from the ATG on *DMXL2* exon 1 is predicted to undergo NMD. D, Schematic representation of the deletion shared in common by cases 8 and 9 from family D, case 10 from family E, and cases 15 and 17 from family F. Genome, The junction sequence of the deletion (a *gray area*) is shown. The fusion has occurred between a LINE 1 repeat sequence (*highlighted with blue*) at intron 1 of *DMXL2* and that at a downstream region of *DMXL2*, with an overlap of a 12-bp segment. mRNA, The sequence of a chimeric gene transcript is delineated. The mRNA structure is the same as that described in the legend for Fig. 3C.

fusion occurred between nonrepeat elements with an overlap of one nucleotide.

All the 5′-RACE products (>500 clones) obtained from LCL and SF of case 3 (family A) and case 4 (family B) were found to be associated with a single exon 1, as observed in control materials. However, PCR amplifications for the 5′-RACE products with a variety of combinations of primers hybridizing to each exon 1 and subsequent sequencing of the PCR products revealed the presence of a chimeric clone consisting of exon I.4 at the 5′ side and exon I.8 at

the 3′ side in both LCL and SF (Fig. 3B). Although such a chimeric clone would have been produced by a splice error, this indicated that duplicated exon 1.4 at the distal nonphysiological position functioned as a transcription start site.

Characterization of the cryptic deletions

In cases from family C, long PCR products were obtained with the P7 primer and the P9 primer, and the deletion junction was determined by direct sequencing with the P8 primer (Fig. 3C). The deleted region was 211,631-bp long and involved exons 2–43 of *DMXL2* and exons 5–10 of *GLDN*. The two breakpoints resided within a LINE 1 repeat sequence and a nonrepeat sequence respectively, and a 33-bp segment with a LINE 1 repeat sequence was inserted to the fusion point. In cases from families D–F, long PCR products were obtained by sequential amplifications with the P12 primer and the P14 primer and with the P13 primer and the P14 primer, and an identical deletion was identified by direct sequencing with the P13 primer (Fig. 3D). The deletion was 165,901-bp long and involved exons 2–43 of *DMXL2*. The fusion occurred between two LINE 1 repeat sequences with an overlap of a 12-bp segment.

Sequence analysis of the 5′-RACE products obtained from LCL of cases 5 and 6 (family C) and from SF of case 9 (family D) and case 10 (family E) revealed the presence of a few clones with *DMXL2* exon 1 (2–5%), together with multiple clones with a single wild-type *CYP19A1* exon 1 (Fig. 3, C and D). Such a chimeric mRNA clone was absent from control materials. Furthermore, *DMXL2* exon 1 was found to be accompanied by a promoter-compatible sequence (Supplemental Fig. 2). This indicated a cryptic usage of *DMLX2* exon 1 as an alternative *CYP19A1* transcription start site in cases with deletions. Notably, because of the presence of the translation start codon on *DMXL2* exon 1, mRNAs of the *DMLX2/CYP19A1* chimeric genes are predicted to produce two proteins, *i.e.* CYP19A1 protein and an apparently nonfunctional 47-amino acid protein with a termination codon on *CYP19A1* exon 2, when the translation started from the initiation codons on *CYP19A1* exon 2 and on *DMLX2* exon 1, respectively. Furthermore, mRNA destined to yield the 47-amino acid protein is predicted to undergo nonsense-mediated mRNA decay (NMD) because it satisfies the condition for the occurrence of NMD (12).

Relative mRNA levels of *CYP19A1* and its neighboring genes

CYP19A1 showed a markedly high expression in the placenta and a relatively weak expression in a limited number of tissues including hypothalamus and ovary. By contrast, *DMXL2* was expressed in a range of tissues with some degree of variation as well as *CGNL1*, *MAPK6*, *TMOD3*, and *TLN2* (Fig. 4).

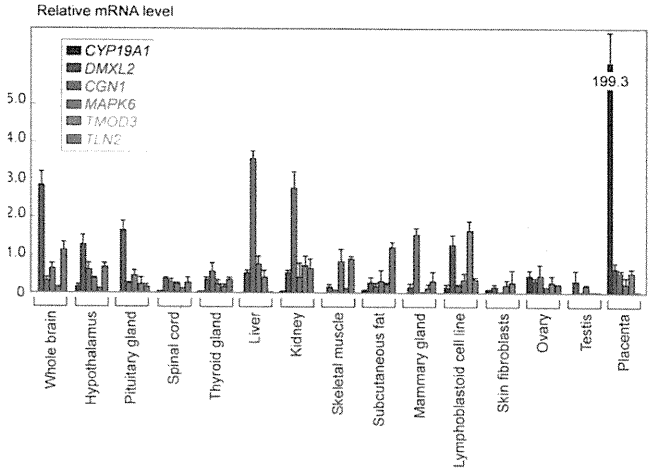

FIG. 4. Expression patterns of *CYP19A1* and the five neighboring genes involved in the chimeric gene formation. Relative mRNA levels against *TBP* are shown.

Discussion

We identified cryptic duplications of the *CYP19A1* promoter region and deletions of the *CYP19A1* upstream region in cases with AEXS. The tandem duplications would have caused *CYP19A1* overexpression because of an increased number of the wild-type transcription start sites. Indeed, because a rare mRNA variant with exon I.4 and exon I.8 was identified, this implies that duplicated exons 1 at the distal nonphysiological position can also function as transcription start sites. Similarly, the deletions would have caused *CYP19A1* overexpression because of a cryptic usage of *DMXL2* exon 1 with a putative promoter function as an extra transcription start site for *CYP19A1*. Indeed, because a few clones with *DMXL2* exon 1 and *CYP19A1* exon 2 were identified, this confirms the formation of a *DMXL2/CYP19A1* chimeric gene. Thus, our results suggest for the first time that duplications of a physiological promoter and deletions of an upstream region can cause overexpression of a corresponding gene and resultant human genetic disease.

Such cryptic genomic rearrangements can be generated by several mechanisms. The tandem duplication in families A and B would be formed by a replication-based mechanism of fork stalling and template switching that occurs in the absence of repeat sequences and is associated with microhomology (13). The deletion in family C is explained by nonhomologous end joining that takes place between nonhomologous sequences and is frequently accompanied by an insertion of a short segment at the fusion point (13).

The deletion in families D–F is compatible with a repeat sequence mediated nonallelic intrachromosomal or interchromosomal recombination (13). Thus, in conjunction with the previously identified four cryptic inversions that are also explainable by fork stalling and template switching or nonallelic recombination (8), genomic sequence around *CYP19A1* appears to harbor particular motifs that are vulnerable to replication and recombination errors.

To date, three types of cryptic genomic rearrangements have been identified in patients with AEXS, *i.e.* duplication type, deletion type (two subtypes), and inversion type (four subtypes) (Fig. 5). Here, although the deletion and the inversion types are associated with heterozygous impairment of neighboring genes (deletion or disconnection between noncoding exon(s) and coding exons), the phenotypes of patients are well explained by excessive *CYP19A1* activity alone. Thus, haploinsufficiency of these neighboring genes would not have a major clinical effect.

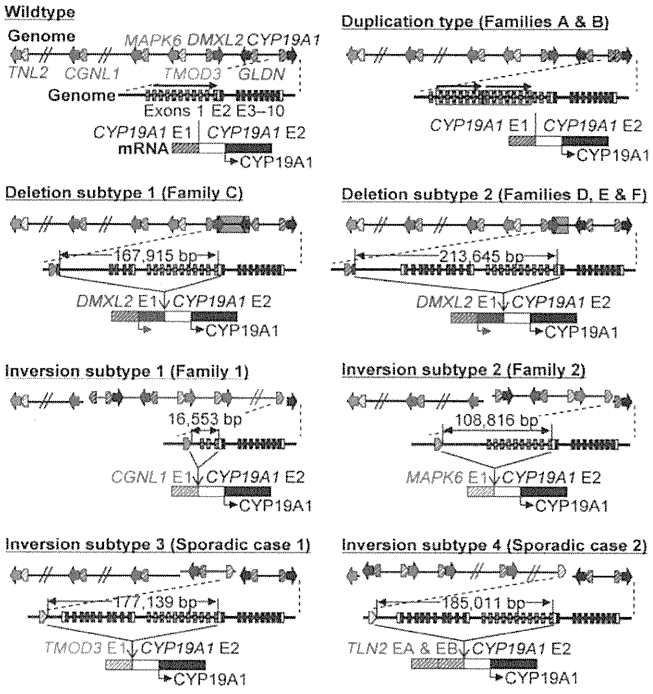

FIG. 5. Schematic representation of the rearranged genome and mRNA structures. The *white* and *black boxes* of *CYP19A1* exon 2 show untranslated region and coding region, respectively (for details, see Supplemental Fig. 1). For the duplication type and the deletion subtypes, see Fig. 3, C and D, for details. For genome, the *striped* and *painted arrows* indicate noncoding and coding exons, respectively (5′→3′). The inverted genomic regions are delineated in *blue lines*. For mRNA, *colored striped boxes* represent noncoding regions of each gene. For *TLN2*, exons A and B correspond to the previously reported exons 1 and 2 (8); because current exon 1 in the public database indicates the first coding exon, we have coined the terms exons A and B for the noncoding exons. The deletion and inversion types are associated with heterozygous impairment of neighboring genes [deletion or disconnection between noncoding exon(s) and the following coding exons]. The inversion subtype 1 is accompanied by inversion of eight of the 11 *CYP19A1* exons 1, and the inversion subtype 2 is associated with inversion of the placenta-specific *CYP19A1* exon I.1.

For the deletion and inversion types, two factors should be considered. One factor is expression patterns of each chimeric gene. In this regard, the five genes involved in the formation of chimeric genes are widely expressed, with some degree of variation (Fig. 4). Furthermore, *in silico* analysis revealed promoter-compatible sequences around exon 1 of *DMXL2*, *CGN1*, *MAPK6*, and *TMOD3* in multiple cell types, although such sequences remain to be identified for noncoding exons of *TLN2* (Supplemental Fig. 2). These findings imply that the chimeric genes show wide expression patterns because expression patterns of chimeric genes would follow those of the original genes.

The other factor is expression dosage of each chimeric gene. In this context, the *DMXL2/CYP19A1* chimeric mRNA was identified only in 2–5% of transcripts from SF, whereas the *CGNL1/CYP19A1* chimeric mRNA and the *TMOD3/CYP19A1* chimeric mRNA accounted for 89–100% and 80% of transcripts from SF, respectively (no data for the *MAPK6/CYP19A1* and the *TLN2/CYP19A1* chimeric genes) (5). This difference is obviously inexplicable by the relative expression level in SF that is grossly similar between *DMXL2* and *TMOD3* and is quite low for *CGNL1* (Fig. 4). In this regard, it is notable that a translation start codon and a following coding region are present on exon 1 of *DMXL2* (Fig. 5). It is likely that *DMXL2/CYP19A1* chimeric mRNA transcribed by the *DMXL2* promoter preferentially recognized the natural start codon on *DMXL2* exon 1 and underwent NMD and that rather exceptional chimeric mRNAs, which recognized the start codon on *CYP19A1* exon 2, were identified by 5′-RACE. By contrast, such a phenomenon would not be postulated for the inversion-mediated chimeric mRNA because of the absence of a translation start codon on the fused exon 1 of *CGNL1* and *TMOD3* (as well as exon 1 of *MAPK6* and exons A and B of *TLN2*) (Fig. 5). For the *CGNL1/CYP19A1* chimeric gene, furthermore, the physical distance between *CGNL1* exon 1 and *CYP19A1* exon 2 is short, and whereas a splice competition may be possible between exon 1 of neighboring genes and original *CYP19A1* exons 1, eight of 11 *CYP19A1* exons 1 including exon I.4 functioning as the major promoter in SF have been disconnected from *CYP19A1*-coding exons by inversion. These structural characters would have also contributed to the efficient splicing between *CGNL1* exon 1 and *CYP19A1* exon 2 (14). In this context, although the *CGNL1/CYP19A1* chimeric gene is associated with functional loss of eight *CYP19A1* exons 1 and the resultant reduction of *CYP19A1* expression in *CYP19A1*-expressing tissues, overall aromatase activity would be increased

by the wide expression of the chimeric gene. These structural properties would primarily explain the difference in the expression dosage of chimeric mRNA between the deletion and the inversion types.

It is inferred, therefore, that the duplication type simply increases *CYP19A1* transcription in native *CYP19A1*-expressing tissues, whereas the deletion and the inversion types cause relatively mild and severe *CYP19A1* overexpression in a range of tissues, respectively. These notions would grossly explain why clinical features of affected males and carrier females and endocrine profiles of affected males are apparently milder in the duplication and the deletion types than in the inversion type and why clinical findings were ameliorated with 1 mg/d of anastrozole in the duplication and the deletion types and with 2–4 mg/d of anastrozole in the inversion type. In addition, the different expression pattern between *CYP19A1* and *DMXL2* may explain, in terms of autocrine and/or paracrine effects, why phenotypic features such as gynecomastia tended to be more severe in the deletion type than in the duplication type under similar endocrine profiles.

Furthermore, several findings are notable in this study. First, a similar degree of FSH-dominant hypogonadotropic hypogonadism is present in the three types, with no amelioration of FSH responses to GnRH stimulation after GnRH priming in two cases with the duplication. This suggests that a relatively mild excess of circulatory estrogens, as observed in the duplication and the deletion types, can exert a strong negative feedback effect on FSH secretion, primarily at the pituitary, as has been suggested previously (15–19). Second, although basal T values appear to be mildly and similarly compromised in the three types, age-matched comparison suggests that T responses to hCG stimulation are apparently normal in the duplication and the deletion types and somewhat low in the inversion type. These data, although they remain fragmentary, would primarily be compatible with fairly preserved LH secretion in the three types and markedly increased estrogen values in the inversion type because T production is under the control of LH (1), and excessive estrogens compromise testicular steroidogenic enzyme activity (20, 21). Lastly, although testis volume appears somewhat small, fertility (spermatogenesis) is normally preserved in the three types. This would be consistent with the FSH-dominant hypogonadotropic hypogonadism because FSH plays only a minor role in male fertility (spermatogenesis) (22). Indeed, males with mutations of *FSHR* encoding FSH receptor as well as mice lacking *FSHB* or *FSHR* can be fertile (23, 24).

The results of this study are contrastive to those of the previous studies. In the previous studies, inversions only have been identified, and each inversion is specific to each family or patient (8). By contrast, in this study, the identical duplication was found in two Japanese families A and B, and the same deletion (subtype 2 in Fig. 5) was shared by three Japanese and one Caucasian families D–F, despite apparent nonconsanguinity. This may be explained by assuming that patients with severe phenotype were preferentially examined in the previous studies, whereas those with the AEXS phenotype were analyzed in this study without ascertainment bias. Furthermore, because phenotypes are milder in the duplication and the deletion types than in the inversion type, this may have permitted the spread of the duplication and the deletion types, but not the inversion type, as the founder abnormalities. This notion predicts that the duplication and the deletion types would be identified by examining patients with mild AEXS phenotype.

In summary, the present study shows that AEXS can be caused by duplications of the physiological promoters and microdeletions of the upstream regions of *CYP19A1* and that phenotypic severity is primarily determined by the tissue expression pattern of *CYP19A1* and the chimeric genes and by structural properties of the fused exons. Most importantly, the present study provides novel models for the gain-of-function mutations leading to human genetic disease.

Acknowledgments

Address all correspondence and requests for reprints to: Dr. Tsutomu Ogata, Department of Molecular Endocrinology, National Research Institute for Child Health and Development, 2-10-1 Ohkura, Setagaya, Tokyo 157-8535, Japan. E-mail: tomogata@nch.go.jp.

Present address for T.O.: Department of Pediatrics, Hamamatsu University School of Medicine, Hamamatsu 431-3192, Japan.

This work was supported by Grants for Research on Intractable Diseases (H22-035 and H22-098) from the Ministry of Health, Labor, and Welfare; Grants-in-Aid for Scientific Research (B) (20390265) and (S) (22227002) from the Japan Society for the Promotion of Science; and Grant-in-Aid for Scientific Research on Innovative Areas (22132004) from the Ministry of Education, Culture, Sports, Science, and Technology.

Disclosure Summary: The authors have nothing to declare.

References

1. **Bhasin S** 2008 Testicular disorders. In: Kronenberg HM, Melmed M, Polonsky KS, Larsen PR, eds. Williams textbook of endocrinology. 11th ed. Philadelphia: Saunders; 645–699
2. **Bulun SE, Takayama K, Suzuki T, Sasano H, Yilmaz B, Sebastian S**

2004 Organization of the human aromatase p450 (CYP19) gene. Semin Reprod Med 22:5–9
3. **Demura M, Reierstad S, Innes JE, Bulun SE** 2008 Novel promoter I. 8 and promoter usage in the CYP19 (aromatase) gene. Reprod Sci 15:1044–1053
4. **Harada N, Utsumi T, Takagi Y** 1993 Tissue-specific expression of the human aromatase cytochrome P-450 gene by alternative use of multiple exons 1 and promoters, and switching of tissue-specific exons 1 in carcinogenesis. Proc Natl Acad Sci USA 90:11312–11316
5. **Shozu M, Sebastian S, Takayama K, Hsu WT, Schultz RA, Neely K, Bryant M, Bulun SE** 2003 Estrogen excess associated with novel gain-of-function mutations affecting the aromatase gene. N Engl J Med 348:1855–1865
6. **Binder G, Iliev DI, Dufke A, Wabitsch M, Schweizer R, Ranke MB, Schmidt M** 2005 Dominant transmission of prepubertal gynecomastia due to serum estrone excess: hormonal, biochemical, and genetic analysis in a large kindred. J Clin Endocrinol Metab 90: 484–492
7. **Martin RM, Lin CJ, Nishi MY, Billerbeck AE, Latronico AC, Russell DW, Mendonca BB** 2003 Familial hyperestrogenism in both sexes: clinical, hormonal, and molecular studies of two siblings. J Clin Endocrinol Metab 88:3027–3034
8. **Demura M, Martin RM, Shozu M, Sebastian S, Takayama K, Hsu WT, Schultz RA, Neely K, Bryant M, Mendonca BB, Hanaki K, Kanzaki S, Rhoads DB, Misra M, Bulun SE** 2007 Regional rearrangements in chromosome 15q21 cause formation of cryptic promoters for the CYP19 (aromatase) gene. Hum Mol Genet 16:2529–2541
9. **Tiulpakov A, Kalintchenko N, Semitcheva T, Polyakov A, Dedov I, Sverdlova P, Kolesnikova G, Peterkova V, Rubtsov P** 2005 A potential rearrangement between CYP19 and TRPM7 genes on chromosome 15q21.2 as a cause of aromatase excess syndrome. J Clin Endocrinol Metab 90:4184–4190
10. **Stratakis CA, Vottero A, Brodie A, Kirschner LS, DeAtkine D, Lu Q, Yue W, Mitsiades CS, Flor AW, Chrousos GP** 1998 The aromatase excess syndrome is associated with feminization of both sexes and autosomal dominant transmission of aberrant P450 aromatase gene transcription. J Clin Endocrinol Metab 83:1348–1357
11. **Bellino FL, Osawa Y** 1977 Localization of estrogen synthetase in the chorionic villus fraction after homogenization of human term placenta. J Clin Endocrinol Metab 44:699–707
12. **Kuzmiak HA, Maquat LE** 2006 Applying nonsense-mediated mRNA decay research to the clinic: progress and challenges. Trends Mol Med 12:306–316
13. **Gu W, Zhang F, Lupski JR** 2008 Mechanisms for human genomic rearrangements. Pathogenetics 1:4
14. **Castillo-Davis CI, Mekhedov SL, Hartl DL, Koonin EV, Kondrashov FA** 2002 Selection for short introns in highly expressed genes. Nat Genet 31:415–418
15. **Shaw ND, Histed SN, Srouji SS, Yang J, Lee H, Hall JE** 2010 Estrogen negative feedback on gonadotropin secretion: evidence for a direct pituitary effect in women. J Clin Endocrinol Metab 95:1955–1961
16. **Belgorosky A, Guercio G, Pepe C, Saraco N, Rivarola MA** 2009 Genetic and clinical spectrum of aromatase deficiency in infancy, childhood and adolescence. Horm Res 72:321–330
17. **Alexander DC, Miller WL** 1982 Regulation of ovine follicle-stimulating hormone β-chain mRNA by 17β-estradiol *in vivo* and *in vitro*. J Biol Chem 257:2282–2286
18. **Mercer JE, Clements JA, Funder JW, Clarke IJ** 1988 Luteinizing hormone-β mRNA levels are regulated primarily by gonadotropin-releasing hormone and not by negative estrogen feedback on the pituitary. Neuroendocrinology 47:563–566
19. **Raven G, de Jong FH, Kaufman JM, de Ronde W** 2006 In men, peripheral estradiol levels directly reflect the action of estrogens at the hypothalamo-pituitary level to inhibit gonadotropin secretion. J Clin Endocrinol Metab 91:3324–3328
20. **Moger WH** 1980 Direct effects of estrogens on the endocrine function of the mammalian testis. Can J Physiol Pharmacol 58:1011–1022
21. **Strauss L, Kallio J, Desai N, Pakarinen P, Miettinen T, Gylling H, Albrecht M, Mäkelä S, Mayerhofer A, Poutanen M** 2009 Increased exposure to estrogens disturbs maturation, steroidogenesis, and cholesterol homeostasis via estrogen receptor α in adult mouse Leydig cells. Endocrinology 150:2865–2872
22. **Kumar TR, Wang Y, Lu N, Matzuk MM** 1997 Follicle stimulating hormone is required for ovarian follicle maturation but not male fertility. Nat Genet 15:201–204
23. **Tapanainen JS, Aittomäki K, Min J, Vaskivuo T, Huhtaniemi IT** 1997 Men homozygous for an inactivating mutation of the follicle-stimulating hormone (FSH) receptor gene present variable suppression of spermatogenesis and fertility. Nat Genet 15:205–206
24. **Layman LC, McDonough PG** 2000 Mutations of follicle stimulating hormone-β and its receptor in human and mouse: genotype/phenotype. Mol Cell Endocrinol 161:9–17

性分化疾患

深見 真紀*

はじめに

ヒトの性分化には，性腺形成を制御する転写因子，ステロイド代謝酵素，性ホルモン受容体，細胞増殖因子などさまざまな因子が関与する．これらの因子をコードする遺伝子の異常は，性分化疾患（Disorders of sex development, DSD）を招く．近年，多数のDSD患者の分子遺伝学的，臨床的解析が行われ，個々の遺伝子異常症の臨床像が明らかとなってきた．さらに，動物実験や *in vitro* 解析によって哺乳類の性分化における新たな遺伝子相互作用が解明された．本稿では，既知遺伝子変異に起因するDSDの臨床像および性分化の分子基盤に関する最近の知見の一部を紹介する．

1 46, XY 核型患者における DSD (46, XY DSD) を招く遺伝子異常症

1）Steroidogenic factor 1 (SF-1) 異常症

近年，多数のSF-1（別名 Ad4Bp，NR5A1）異常症患者が報告され，本症が46, XY DSDの原因疾患として重要であることが明確となった[1]．また，本症患者の臨床的多様性が明らかとなった．*SF-1* は，1990年代に単離された遺伝子で，副腎と性腺の形成と機能の様々な段階に関与することが知られている．SF-1は，組織特異的に発現する核内転写因子であり，標的遺伝子のプロモーターまたはエンハンサーに直接結合してその転写を調節する．SF-1標的遺伝子には，性腺形成に関与する因子（*DAX1*，*SOX9*），ゴナドトロピン分泌調節に関与する因子（*GnRH*，*GnRH受容体*，*FSHβ*，*FSH受容体*）およびステロイド合成酵素（*CYP11A1*，*STAR*，*HSD3B2*）など，多数の遺伝子が含まれる．*SF-1* の機能低下変異は，これら標的遺伝子の発現異常を招く．なお，変異陽性患者の大多数は，*SF-1* の機能低下または機能喪失変異をヘテロ接合性に有するが，ミスセンス変異をホモ接合性に有する症例も報告されている[1]．*SF-1* の変異は遺伝子全体に分布しており，DNA結合領域に多く認められる．

SF-1 遺伝子変異は，46, XY 患者において，子宮を有する女性型表現型から尿道下裂と停留精巣のみを呈する男性型表現型までさまざまな重症度のDSDを招く[1]．同様に，精巣の形態はほぼ正常から重度の異形成または低形成まで幅がある．SF-1異常症の正確な発症頻度は不明であるが，性腺異形成を伴う46, XY DSD患者の15％に *SF-1* の異常が同定されたとの報告がある[1]．また，Philibertらは，テストステロン低値を呈する46, XY 原発性無月経患者15例を解析し，5例において *SF-1* 遺伝子変異を同定した[2]．この成績は，出生時に46, XY DSDと診断される新生児のみならず，思春期以降に原発性無月経によって見出される46, XY 核型女性患者においても，*SF-1* 遺伝

*独立行政法人国立成育医療研究センター 分子内分泌研究部
Maki Fukami : Disorders of sex development. Department of Molecular Endocrinology, National Research Institute for Child Health and Development.

子異常が存在する可能性を示唆する．一方，性腺機能異常を伴わない副腎機能低下症患者では，*SF-1* 遺伝子変異の頻度は著しく低いと推測されている[3]．また，*SF-1* 変異陽性 DSD 患者のなかで，副腎不全症状を認める症例は比較的少数である[1]．したがって，*SF-1* 半量不全患者において副腎の形成はある程度保持されると推測される．

SF-1 遺伝子変異は，46, XY DSD のみならず，46, XX 患者における卵巣機能不全を招く．*SF-1* 変異陽性女性では，原発性または続発性無月経が認められる．しかし，正常卵巣機能を有する変異陽性女性が多く報告されていることから，SF-1 は卵巣よりも精巣において重要な役割を果たしていることが示唆される[1]．

2）アンドロゲン受容体（AR）異常症

AR 異常症は，46, XY DSD を招く単一遺伝子異常症の中でもっとも頻度が高い病態である[4]．とくに，完全な女性型外性器と血中テストステロン高値を呈する 46, XY 症例では，過半数において *AR* 変異が同定される．これまでに多数の患者が報告され，本症の分子遺伝学的，臨床的特徴が明らかとなった[4]．本症は，完全な女性型表現型を呈する症例から不妊症の男性まで，幅広い臨床スペクトラムを有する．

AR は，X 染色体上に位置する遺伝子であり，男性では 1 コピーの *AR* の機能喪失により DSD が生じる．*AR* 遺伝子変異は，翻訳領域全体に広く分布し，ミスセンス，ナンセンス，フレームシフト，スプライス異常など多くの変異パターンを含む[4]．最近の研究では，エクソン 1 に多くの変異が存在することが見出されている[4]．変異の種類と位置は，患者の表現型の重症度に関連すると推測される．さらに，*AR* 遺伝子エクソン 1 の非翻訳領域には (CAG) n 反復配列多型が存在し，その数の差が同一変異陽性患者間の疾患重症度の差の一因である可能性が見出されている．

3）Chromobox homolog 2（CBX 2）異常症

CBX2 は，2009 年にはじめてヒト 46, XY DSD への関与の可能性が見出された遺伝子である[5]．従来，*CBX2* のマウス相同遺伝子 *M33* は，DSD 発症責任遺伝子であると推測されていた．これは，*M33* が形態形成に関与するポリコーム遺伝子群に属すること，および，ノックアウトマウスオスの 50 ～ 75 %で女性型内外性器の形成が認められることに基づく．Biason-Lauber らは，DSD 患者を対象として *CBX2* の変異解析を行い，完全女性型外性器と卵巣を有する 46, XY 患者において，複合ヘテロ接合性変異を同定した[5]．さらに彼らは，野生型 CBX 2 は *in vitro* で *SF-1* の転写を活性化するが，患者で同定された変異型 CBX 2 はこのような転写活性化能を喪失していることを見出した．以上の成績は，*CBX2* がヒトの性分化カスケードにおいて *SF-1* の上流に位置し，その機能喪失性変異が常染色体劣性遺伝形式の 46, XY DSD を招く可能性を示唆する．しかし，患者で同定された変異はいずれもミスセンス変異であるため，まれな多型である可能性は否定できない．今後さらなる患者解析が必要である．

2 46, XX DSD を招く遺伝子異常症

1）R-spondin 1（RSPO 1）異常症

46, XX DSD の原因としては，これまでに，先天性副腎酵素欠損症，染色体構造異常による *SRY* の獲得，*DAX1* や *WNT4* の異常などが知られている．一方，これらの異常を伴わない患者，とくに精巣組織を有する *SRY* 陰性 46, XX 患者における疾患発症機序はほとんど解明されていなかった．

2006 年，*RSPO1* がこのような 46, XX DSD の発症責任遺伝子であることが明らかとなった[6]．Parma らは，多数の患者を有する近親婚 2 家系の解析から，*RSPO1* 近傍の座位が 46, XX DSD と連鎖することを見出し，患者において *RSPO1* ホモ接合性変異を同定した．RSPO 1 は，成長因子であり，βカテニンの安定化または WNT シグナルの活性化を介して卵巣の形成に関与すると推測される．この成績は，単一遺伝子の機能喪失変異が，*SRY* 非存在下で 46, XX 個体における精巣の形成と内外性器の男性化を招きうることをはじ

めて明確とするものである．一方，*RSPO1*変異をホモ接合性に有する46, XY男性は正常妊孕性を保持していることから，RSPO 1は精巣機能には必須でないと推測される．なお，*RSPO1*は皮膚においても強く発現しており，変異陽性患者では，DSDに加え，皮膚の角化異常と扁平上皮癌の易罹患性が認められる[6]．最初の報告の後46, XX卵巣精巣性DSD (46, XX ovotesticular DSD) 患者においても*RSPO1*変異が同定され，*RSPO1*変異がさまざまな重症度の46, XX DSDを招くことが明らかとなった[7]．

3 46, XY DSDと46, XX DSDを招く遺伝子異常症

1）チトクローム P450 オキシドレダクターゼ (POR) 異常症

POR異常症は，2004年に疾患概念が確立された劣性遺伝病であり，先天性副腎酵素欠損症の一つに位置づけられる．最初の変異陽性患者が報告されてから5年間に60例以上の患者が相次いで報告され，本疾患が先天性副腎酵素欠損症の中で，比較的頻度の高い病態であることが明らかとなった．本症では，男女共に出生時の外性器異常を認めることが重要な点である．すなわち，女児では陰核肥大，陰唇融合，共通尿生殖洞などの男性化が，男児では尿道下裂，停留精巣，マイクロペニスなどの男性化不全が認められる（**図1**）[8, 9]．なお，*POR*変異陽性患者では，DSDに加え，骨形成異常，副腎不全，妊娠中母体男性化など多彩な臨床症状が認められる．これは，PORが50種類以上の酵素の活性化に関与する補酵素であることによって説明される．

POR異常症の外性器異常の発症には，ステロイド産生異常とビタミンA代謝異常の2つの要因が関与すると推測される．ステロイド産生異常としては，1) 胎盤アロマターゼ (CYP19A1) 活性低下に起因する男性ホルモン蓄積，2) 胎児期・新生児早期特異的男性ホルモン産生経路（backdoor pathway）における男性ホルモン過剰産生，3) 胎児精巣におけるCYP17A1活性低下による男性ホルモン産生障害が関与すると推測される（**図2**）．なお，これらのうち，胎盤とbackdoor pathwayにおける男性ホルモン産生は出生後に消失するため，出生後の女児男性化の進行はない．思春期には，男女ともに性腺におけるホルモン産生障害を反映する二次性徴の出現不全を認める．ビタミンA代謝異常としては，POR依存性ビタミンA代謝酵素 (CYP26A1, B1, C1) の活性低下に起因する活性型ビタミンA（all-trans retinoic acid, atRA）蓄積が関与すると推測される[10]．この仮説は，POR異常症患者において，atRAによる器官形成障害に一致する腎泌尿器・下部消化管奇形が高頻度に認められること，血中atRA濃度が正常上限から高値であることによって支持される[10]．

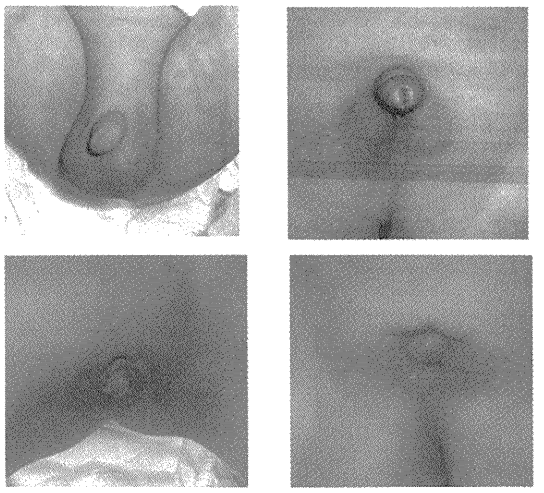

図1 POR異常症患者の外性器（文献8, 9より引用, 改変）：POR異常症は，46, XY DSDと46, XX DSDを招く疾患である．なお，日本人患者では，比較的男性外性器異常の頻度が低く，女性外性器異常の頻度が高いと推測される．すなわち，男性においては正常男性型外性器（左上段）またはマイクロペニスや停留精巣（左下段）が認められ，女性ではほぼ全例に陰核肥大や陰唇融合などの男性化（右）が認められる．これは，本邦においてCYP17A1に対する残存活性が低い人種特異的変異が高頻度に認められることによって説明される．

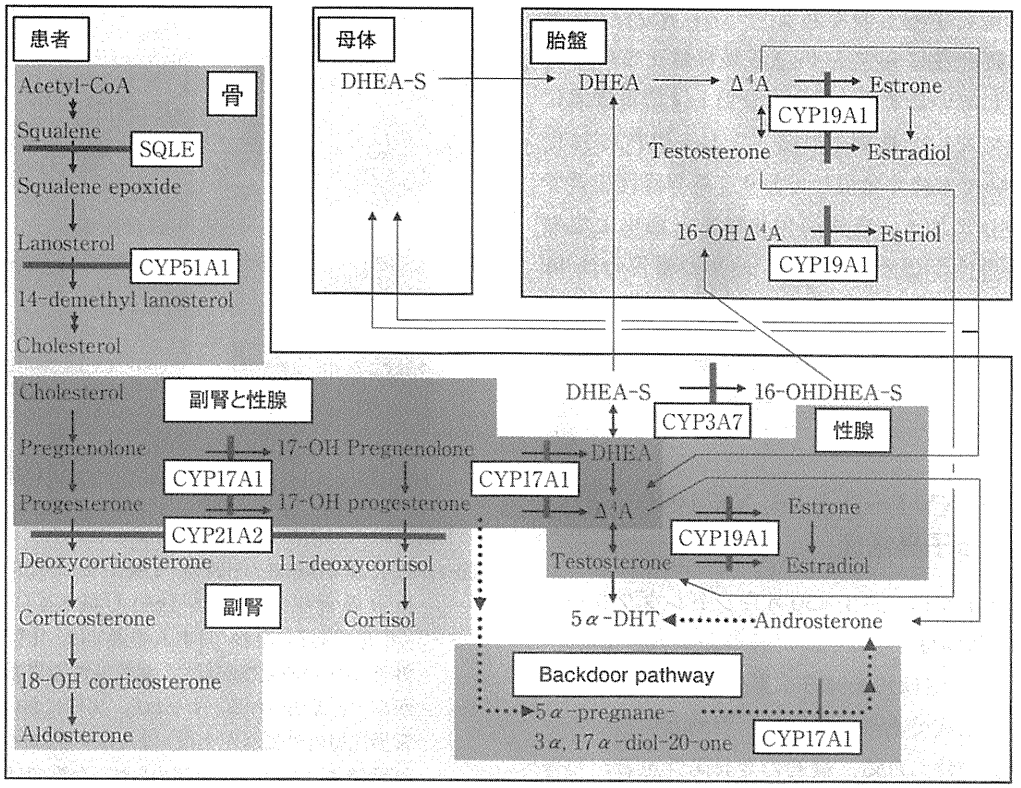

図2　POR 異常症におけるコレステロール，ステロイド代謝異常（文献8より引用，改変）：
POR 異常症では，骨，副腎，性腺，胎盤における POR 依存性酵素の活性低下に起因する骨形成障害，DSD，妊娠母体男性化が認められる．46, XY DSD の発症には精巣 CYP17A1 活性低下によるアンドロゲン産生低下が，46, XX DSD の発症には胎盤 CYP19A1 活性低下によるアンドロゲン蓄積と backdoor pathway 由来の dihydrotestosterone 過剰産生が関与していると推測される．

なお，POR 異常症の変異パターンには人種差があり，本邦においては全変異アリルの 70 %以上を人種特異的創始者変異である R457H が占める[8]．一方，欧米人患者で多く報告されている A287P はこれまで日本人患者では同定されていない．このような変異パターンの差は，臨床症状の重症度の人種差を招く．とくに，日本人患者では欧米人に比較して女性外性器異常の頻度が高く，男性外性器異常の頻度が低いと推測される．これは，R457H 変異体が，CYP19A1 と CYP17A1 に対し比較的低い残存活性を有することに一致する．

4 哺乳類の性分化に関する新たな知見

近年，マウスの研究から，性分化の分子基盤に関する 2 つの重要な知見が得られた（**図3**）．これらは，ヒトの DSD 発症メカニズムの理解に役立つと考えられる．第一に，精巣形成を制御する遺伝子相互作用が解明された[11]．すなわち，精巣形成の基盤となるセルトリ細胞の分化が *Sox9* の持続的発現に依存することが見出され，さらにこの *Sox9* の発現を発生時期特異的に制御する転写因子が明らかとなった：1) 10.5 dpc までの精巣分化初期における基礎的転写は Sf-1 に依存する，2) 11.0 dpc 前後に Sry と Sf-1 による強い転写誘導が生じる，3) その後，Sf-1 と Sox9 自身および

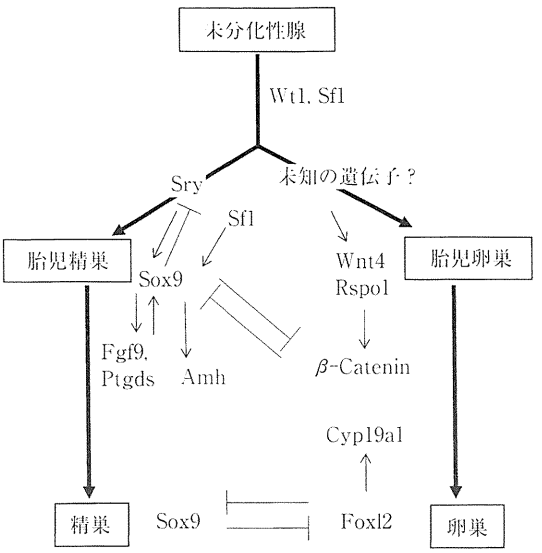

図3 哺乳類の性腺の分化と維持に関与する遺伝子相互作用
精巣の分化と維持にはSox 9が中心的役割を果たすと推測される．卵巣の分化を支配する因子は依然不明な点が多い．卵巣の維持にFoxl 2が関与することが最近の研究で明らかになった．
このモデルは，マウスにおいて解明された[11～13]．
ヒトにおける性分化の分子基盤に関しては今後の検討が必要である．

Fgf 9などの因子によって強い発現が維持される．このような転写制御は，Sry，Sf-1，Sox 9が*Sox 9*精巣特異的エンハンサー（TES）へ直接結合することによって生じると推測される．なお，上記2）のSryによる*Sox 9*誘導に関して，Hiramatsuらは，11.0－11.25 dpcのわずか6時間における*Sry*の発現が精巣形成を決定することを見出している[12]．性決定因子Sryの主要な生体内機能は，この時期の*Sox 9*の発現誘導であると推測される．一方，*Sry*の発現が12.0 dpcに消失するにもかかわらず*Sox 9*の発現は持続することから，Sryは*Sox 9*の発現誘導には必須であるが，発現維持に関与しないことが明らかである．なお，46, XX個体では，46, XY個体と同様にSf-1による*Sox 9*の基礎的転写が生じるが，その後*Sox 9*の発現が抑制される．この*Sox 9*抑制機構は充分解明されていないが，下記のFoxl 2などが関与すると推測される．

第二に，卵巣形成の可逆性が明らかとなった．従来，性腺の分化は*SRY/Sry*の有無に依存し，*SRY*が存在するときは精巣への分化が生じ，存在しないときは受動的に卵巣が形成されると考えられていた．しかし，2009年，Uhlenhautらは，成獣46, XXマウスで*Foxl 2*の機能を喪失させた場合，*Sry*が存在しないにもかかわらず卵巣組織の形態が精巣様に変化することを見出した[13]．さらに，このマウスの性腺は，正常精巣に類似した遺伝子発現パターンと男性ホルモン産生能を有していた．この成績は，正常46, XX個体において卵巣の形態と機能を維持するための機構が生涯にわたり機能しており，この機構の破綻が*Sry*非依存性に成獣期卵巣の精巣への再分化を招くことを示

唆する．この卵巣維持機構の中心は，Foxl 2 による *Sox9* の抑制であると推測される．今後，ヒトの卵巣機能における FOXL 2 の役割について検討が必要である．

おわりに

性分化は，様々な遺伝子が関与する複雑な過程である．既知遺伝子の変異が同定されない DSD 患者が多く報告されていることから，DSD の発症には多数の未知遺伝子が関与すると推測される．また，DSD は，単一遺伝病のほか，多因子遺伝病およびインプリンティング異常症として発症することが知られている．今後，モデル動物の解析や患者の網羅的変異解析などにより，DSD の発症メカニズムに関する研究が急速に進展すると期待される．

文　献

1) Köhler, B., et al.: Minerva Endocrinol., 35 (2): 73, 2010.
2) Philibert, P., et al.: Reprod. Biol. Endocrinol., 8 (1): 28, 2010.
3) Lin, L., et al.: Sex. Dev., 2 (4-5): 200, 2008.
4) Audi, L., et al.: J. Clin. Endocrinol. Metab., 95 (4): 1876, 2010.
5) Biason-Lauber, A., et al.: Am. J. Hum. Genet., 84 (5): 658, 2009.
6) Parma, P., et al.: Nat. Genet., 38 (11): 1304, 2006.
7) Tomaselli, S., et al.: Hum. Mutat., 29 (2): 220, 2008.
8) Fukami, M., et al.: J. Clin. Endocrinol. Metab., 94 (5): 1723, 2009.
9) Fukami, M., et al.: Pediatr. Res., 59 (2): 276, 2006.
10) Fukami, M., et al.: Mol. Genet. Metab., 100 (3): 269, 2010.
11) Sekido, R., et al.: Trends Genet., 25 (1): 19, 2009.
12) Hiramatsu, R., et al.: Development, 136 (1): 129, 2009.
13) Uhlenhaut, N. H., et al.: Cell, 139 (6): 1130, 2009.

特集　コピー数変異

小児内分泌疾患とゲノムコピー数異常

深見真紀　緒方　勤

生　体　の　科　学
第62巻　第6号 別刷
2011年12月15日 発行

（財）金原一郎記念医学医療振興財団／医学書院

生体の科学　62(6)：546-551，2011

特集　コピー数変異

小児内分泌疾患とゲノムコピー数異常

深見真紀　緒方　勤

近年，分子遺伝学的解析技術の進歩に伴い，ゲノムコピー数異常が容易に検出されるようになった。これにより，さまざまな単一遺伝子異常症において疾患発症の原因となる微小欠失や重複が同定された。このようなコピー数異常には遺伝子翻訳領域を包含する欠失や重複だけでなく，翻訳領域から離れた領域の異常が含まれる。本稿では，コピー数異常に起因する小児内分泌疾患の例として，SHOX異常症とアロマターゼ過剰症について概説する。

1　SHOX異常症(レリーワイル症候群)

性染色体短腕擬常染色体領域に位置する遺伝子*SHOX*は，骨細胞特異的に転写活性化作用を発揮する核内転写因子をコードしている[1]。*SHOX*はX不活化を受けず，男女ともに2コピーの活性型で存在する。1コピーの*SHOX*の機能喪失(半量不全)は低身長，ターナー骨格徴候，レリーワイル症候群(LWD)の原因となる。LWDは四肢短縮と前腕マデルング変形を主徴とする先天性骨形成異常症であり，これまでに200例以上の患者が報告されている。

われわれはこれまでに，典型的なLWDを呈する日本人患者29家系50例の解析を行い，本症の分子遺伝学的異常を明らかとしている(図1)[2]。とくに重要な知見として，下記の3点が挙げられる。

第1に，LWD患者における遺伝子異常の主体は遺伝子内点変異ではなく微小欠失である。これは，29家系のうち*SHOX*遺伝子内点変異を有する家系が5家系のみであり，21家系は微小欠失を有していたことに基づく。なお，これらの欠失は2 Mbp以下であり，通常の細胞遺伝学的検査では

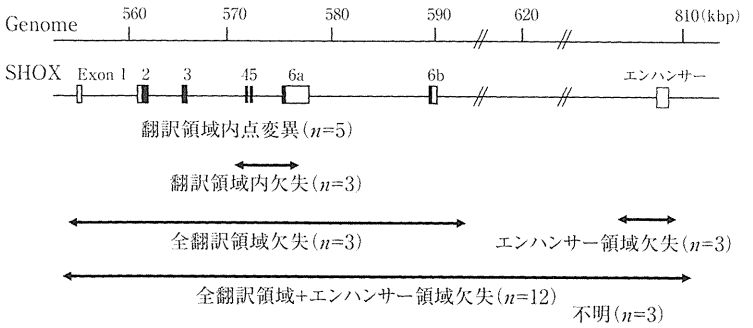

図1　日本人レリーワイル症候群患者29家系における遺伝子異常

Pediatric endocrine disorders and copy number abnormalities
Maki Fukami：国立成育医療研究センター 分子内分泌研究部(〒157-8535 東京都世田谷区大蔵2-10-1)
Tsutomu Ogata：浜松医科大学 小児科(〒431-3192 静岡県浜松市半田山1-20-1)

0370-9531/12/¥500/論文/JCOPY

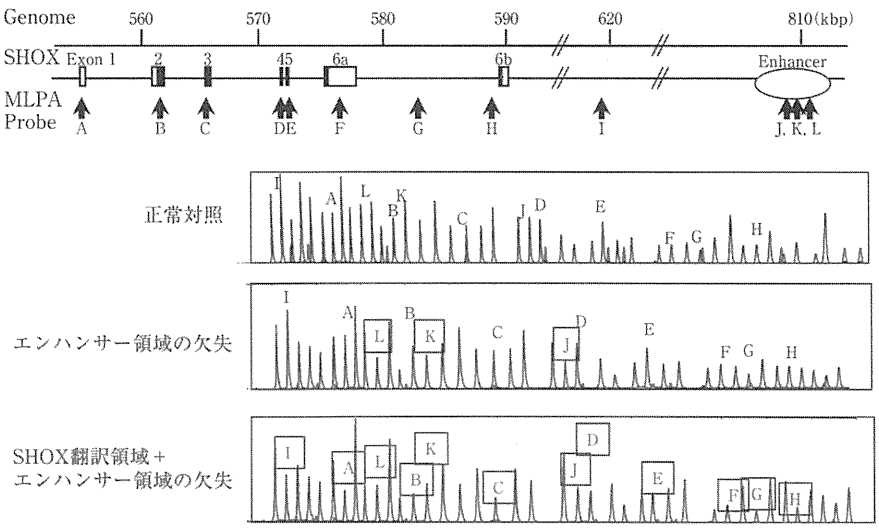

図2　レリーワイル症候群患者における multiple ligation probe amplification(MLPA)法による欠失の同定
四角で囲ったプローブのピークの減少が認められ，この領域を包含するヘテロ接合性欠失が示唆される。

同定不可能であった。大部分の症例の欠失は，*SHOX* 翻訳領域を包含するコスミドをプローブとしたFISH解析または*SHOX*遺伝子上流の(CA)n多型を利用したマイクロサテライト解析で同定された。一方，3例において認められた遺伝子内微小欠失は，multiple ligation probe amplification(MLPA)法によってはじめて同定可能であった(図2)。さらに最近，より感度の高い方法としてアレイ comparative genomic hybridization (CGH)法が用いられるようになった。MLPA法とアレイCGH法は患者のゲノムDNAのみを用いて微小欠失の同定が可能であることから，SHOX異常症のような欠失主体の疾患のスクリーニング法としてきわめて有用である。

第2に，LWD患者における微小欠失のサイズと位置はさまざまである。切断点の塩基配列解析から，これらの欠失の発症には相同配列間での組換え異常(non-allelic recombination)，および，non-homologous end-joining(NHEJ)の両者が関与することが示唆されている(図3)。これは，*SHOX* が存在する性染色体擬常染色体領域において高頻度に組換えが生じること，また，*SHOX* 周辺に *Alu* などの反復配列が多く存在することによって説明される。反復配列は直接的に組換え異常の原因となるのみならず，NHEJの発症リスクを高めると考えられる。

第3に，LWD患者の遺伝子異常には*SHOX*翻訳領域から離れた部位の微小欠失が含まれる。この欠失領域内には*SHOX*の骨特異的発現を支配するエンハンサーが存在し，このエンハンサーの機能喪失がほぼ完全な*SHOX*発現消失を招くと予想される。現在，このエンハンサーの存在部位は*SHOX*翻訳領域から3'側に約250-300 kbp離れた約10 kbpの範囲に限局化されている。しかし，翻訳領域の下流に存在するエンハンサーが*SHOX*発現を制御する機序は解明されていない。

なお，LWD患者における微小欠失のパターンには人種差が存在する可能性がある。われわれが行った日本人患者の解析では，全翻訳領域とエンハンサー領域をともに包含する欠失が最も高頻度であった(図1)。一方，スペインからはエンハンサー領域に限局した微小欠失の頻度が最も高いとの報告がなされている。今後，多数の患者の解析により，個々の人種における微細欠失のパターンが明らかとなると期待される。このような知見は人種特異的多型の解明につながる可能性がある。

2　アロマターゼ過剰症

アロマターゼ過剰症(AEXS)はアロマターゼ遺

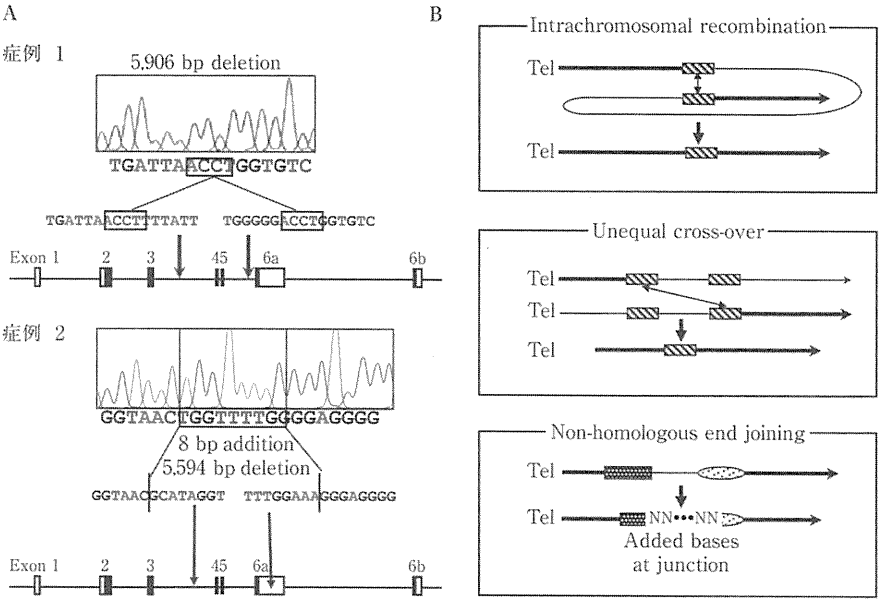

図 3　レリーワイル症候群患者2例における切断点の塩基配列解析

SHOX 欠失の発症には組換え異常および non-homologous end-joining の両者が関与することが示唆される。

伝子(*CYP19A1*)の過剰発現に起因するまれな常染色体優性遺伝疾患である。アロマターゼは男性ホルモン(アンドロゲン)を女性ホルモン(エストロゲン)へと変換するミクロゾーム酵素である。AEXSを有する男性患者ではエストロゲン過剰産生を反映して，乳房腫大，骨年齢促進，性腺機能不全が認められる。女性患者の多くは無症状であるが，一部の症例では月経不順や思春期早発が生じる。2003年，Shozuらおよび Demuraらにより，AEXS 2家系と2孤発例において，アロマターゼ遺伝子上流の染色体逆位が同定された[3,4]。このような逆位陽性患者では，*CYP19A1* と近隣に位置する広範囲発現遺伝子の間でキメラ遺伝子が形成されることにより，アロマターゼ過剰発現が生じると推測される。

2011年，われわれは6家系18例(家系A-F)のAEXS患者の解析を行い，本症の原因となる新たなコピー数異常を同定した[5]。家系AとBでは，*CYP19A1* 翻訳領域から10,983 bp離れた領域に79,156 bpの大きさのタンデム重複が同定された(図4A，B)。この領域は，*CYP19A1* の非翻訳エクソン1(組織特異的プロモーター)11個のうちの七つ(エクソンⅡa，I.8，I.4，I.5，I.7，If，I.2)を包含していた。この重複の fusion point は反復配列外にあり，1塩基の相同性を有していた。mRNA解析では *CYP19A1* エクソン1のうちの一つを有する正常なクローンのほかに，5'側にエクソンI.4，3'側にエクソンI.8が結合したクローンが得られた(図4C)。このクローンはスプライスエラーによって生じた産物であると推測される。このようなキメラクローンの存在は，非生理的な位置に存在する遠位のプロモーターからも転写が生じていることを示すものである。したがって，家系AとBでは *CYP19A1* プロモーター数の増加によって転写効率が増加し，アロマターゼ遺伝子過剰発現が生じたことが示唆される。

家系Cでは *CYP19A1* スタートコドンから141,758 bp離れた領域に211,631 bpの欠失が同定された(図5A，B)。この欠失は隣接遺伝子 *DMXL2* エクソン2-43と *GLDN* エクソン5-10を包含していた。この欠失の切断点は，一方はLINE 1配列内，他方は反復配列外にあり，33塩基の由来不明の塩基配列の挿入を伴っていた。mRNA解析では *CYP19A1* エクソン1のうちの一つを有する正常クローンのほか，*DMXL2* エクソン1と *CYP19A1* エクソン2を含む *DMXL2-CYP19A1* キメラクローンが得られた(図5C)。

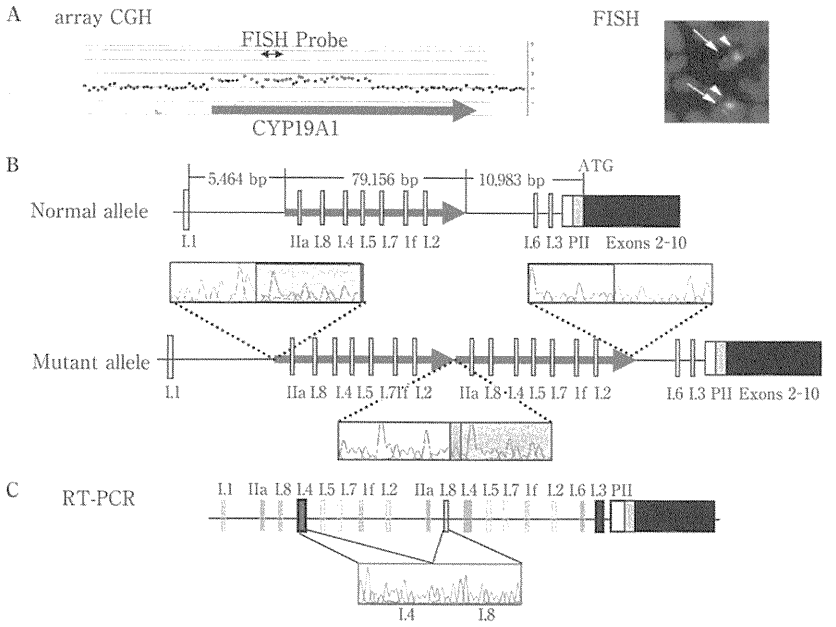

図 4　アロマターゼ過剰症家系 A と B における遺伝子異常

A：アレイ CGH 解析(左)と FISH 解析(右)。*CYP19A1* のプロモーター領域のヘテロ接合性重複が同定された。B：ゲノム構造異常。*CYP19A1* エクソン 1 のうち七つを包含するタンデム重複。Fusion point は反復配列外にあり，1 塩基の相同性を有する。C：mRNA 解析。5′側にエクソン I.4，3′側にエクソン I.8 が結合した mRNA クローンが同定された。このクローンの存在は遠位に増えたエクソン I.4 からも転写が生じていることを示唆する。

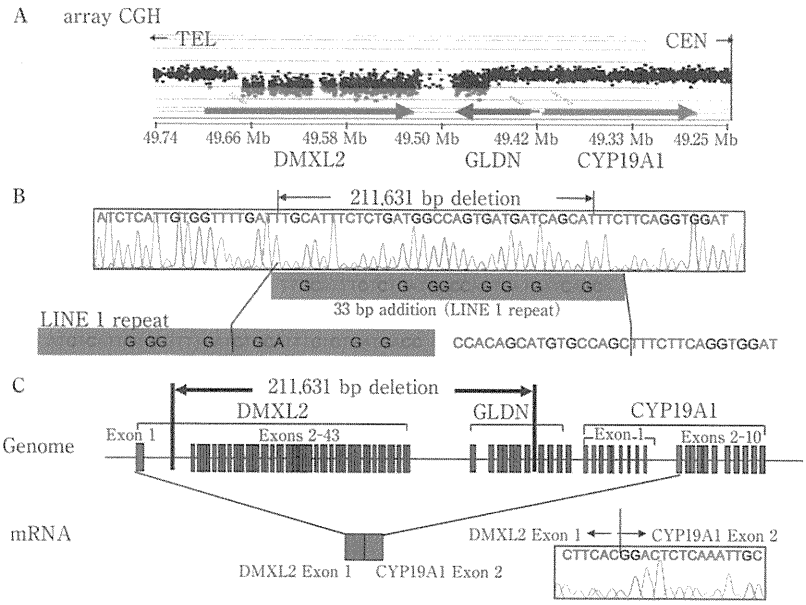

図 5　アロマターゼ過剰症家系 C における遺伝子異常

A：アレイ CGH 解析。*CYP19A1* 上流領域のヘテロ接合性欠失が同定された。B：ゲノム構造異常。*DMXL2* エクソン 2-43 と *GLDN* エクソン 5-10 を包含する欠失が同定された。切断点は一方は LINE 1 配列内，他方は反復配列外にあり，33 塩基の由来不明の塩基配列の挿入を伴う。C：mRNA 解析。*DMXL2-CYP19A1* キメラ mRNA クローンが同定された。